

Correlation Coefficient Measure of Mono and Multimodal Brain Image Registration using Fast Walsh Hadamard Transform

D.Sasikala and R.Neelaveni

Abstract—A bundle of image registration procedures have been built up with enormous implication for data analysis in medicine, astrophotography, satellite imaging and little other areas. An approach to the problem of mono and multimodality medical image registration is proposed, with a fundamental concept Correlation Coefficient, as a matching measure. It measures the statistical dependence or information redundancy between the image intensities of corresponding voxels in both images. Maximization of CC is a very broad and dominant norm. As no assumptions are made regarding the nature of this dependence and no limiting constraints are imposed on the image content of the modalities involved. The accuracy of the CC criterion is validated for rigid body registration of computed tomography (CT), and magnetic resonance (MR T1 and T2) images by comparison with the registration solution. Experimental results prove that subvoxel accuracy with the reference solution can be achieved completely automatically without any preprocessing steps that make this process ensemble for medical applications.

Index Terms—Image Registration, Mono and Multimodal Brain Images, Walsh Transform, Fast Walsh Hadamard Transform, Correlation Coefficient.

I. INTRODUCTION

Digital image processing is developing the eventual machine that could carry out the visual functions of all. It is a swiftly budding field with developing applications in many areas of Science and Engineering. The most important principle of registration is to combine the sets of data with the variants if any or with their similarities into a single data. These sets of data are got by sampling the identical scene or object at different times or from different perspectives, in different co-ordinate systems. The intention of registration is to envision a single data merged with all the details about these sets of data obtained at different times or perspectives or co-ordinate systems. Such data is very crucial in medicine for doctors to prepare for surgery. The most general and significant classes of image analysis algorithm with medical applications [1,3] are image registration and image segmentation. In image analysis procedure, the same input gives out somewhat detail sketch of the scene whose image is being considered. Hence the image analysis algorithms

execute registration as a part of it headed for generating the depiction. In solitary subject analysis, the statistical analysis is made either prior to or subsequent to registration. But in group analysis, it is completed subsequent to registration.

Commonly registration is the most complex task, as aligning images to have common characteristics by general features and differences if any are to be stressed for immediate visibility to the naked eye. There is no universal registration [1-17] algorithm that can work reasonably well for all images. An appropriate registration algorithm for the particular problem must be chosen or developed, as they are adhoc in nature. The algorithms can be integrated explicitly or implicitly or even in the form of a various of factors. This step establishes success or failure of image analysis. This procedure may be classified based on four different aspects given as follows: (i) the feature selection (extracting features from an image) using their similarity measures and a correspondence basis (ii) the transformation function (iii) the optimization procedure and (iv) the model for processing by interpolation.

Amongst the various algorithms developed for image registration so far, techniques based on image intensity values are particularly outstanding as they are easy to mechanize as solutions to optimization problems. Pure translations, for example, can be estimated proficiently and universally as the maxima of the cross correlation function between two images [11] [15] [17]. Additional commands such as rotations, combined with scaling, shearing, give rise to nonlinear functions which must be determined using iterative nonlinear optimization methods [11].

In the Medical Imaging Field, image registration is normally used to merge the complementary and synergistic information of images accomplished from multi modalities. A problem when registering image data is that one does not have direct access to the density functions of the image intensities. They must be predictable from the image data. A variety of image registration procedures have been exercised for successfully registering images that are unoccluded and commonly performed with the use of Parzen Windows or Normalized Frequency Histograms [12].

The work proposed in this paper employs Correlation Coefficient measure for mono and multimodal image registration using Fast Walsh Hadamard Transform (FWHT) [18, 19, 20]. The coefficients acquired are normalized to find out a unique number which in turn stands for the numerals in a particular range. The tests conducted on clinical images show that proposed algorithm performed well than the conventional Walsh Transform (WT) method in Medical

Manuscript received November 17, 2010

D.Sasikala is Assistant Professor, Department of Computer Science and Engineering, Bannari Amman Institute of Technology, Sathyamangalam, Tamil Nadu, INDIA-638401 (anjansasikala@gmail.com)

R.Neelaveni, Associate Professor, Department of Electrical and Electronics Engineering, PSG College of Technology, Coimbatore, Tamil Nadu, INDIA -641004. (rn64asok@yahoo.co.in).

Image Registration. In addition, this paper gives a comparative analysis of Correlation Coefficient [15] measure for mono and multimodal image registration.

The rest of the paper is organized as follows. Section 2 gives an overview on the related work for Correlation Coefficient measure for image registration. Section 3 gives details about Correlation Coefficient measure for image registration using WT. Section 4 describes the proposed approach about Correlation Coefficient measure for image registration using FWHT. Section 5 illustrates the experimental results and Section 6 concludes the paper with a discussion.

II. RELATED WORK

Many discussions have been carried out previously on Image Registration. This section of paper provides an immediate look on the significant research work in Correlation Coefficient measure for image registration.

Sullivan, D.R and his team [21] presented a high-speed compact digital correlation tracker which determines the frame-to-frame translational motion between two images. Holden, M et al. [22] Proposed a rank correlation coefficient with assessed difference images. Inglada, J. and his group [23] introduced similarity measures which can replace the correlation coefficient in a deformation map estimation scheme. Anthony, A with his team[24] compared the reliability of mutual information, correlation coefficient and sum of absolute differences as similarity metrics using search data strategy. They also put forward a measure, called alignability. Lazaridis, G. and his colleagues [25] suggested a new algorithm which can be used to register images of the same or different modalities. Lee and his colleagues [26] found that the contribution on overlay error budget can be quantitatively analyzed in terms of the correlation among registration errors of the reticle. Singh. M. and his team [27] reported a method to co-register in-vivo MRIs to microscopic examinations of histological samples drawn off the postmortem brain. Xiaojin Shi and his group [28] put forward a new definition of correlation coefficient to improve the calculation accuracy of offset between two images. Chatelain. F. et al [29] evaluated the potential interest of using bivariate gamma distributions for image registration and change detection. Bing Luo and his team [30] presented that using projection of wavelet decomposition coefficients instead of mutual correlation can simplify the calculation from 2D to 1D. Ito. I and his team [31] presented a subpixel estimation technique for DCT sign phase correlation (DCT-SPC). Jichao Jiao et al. [32] proposed an astronomical image registration based on the nonsubsampling contourlet transform (NSCT) and a new evaluation criterion to estimate the results of the registration. Miaoqing Huang and his group [33] put forward rigid-body transformation on the test image to register it with the reference image; and correlation coefficient is used as the similarity metric between the two images. Two different algorithms, exhaustive search algorithm and discrete wavelet transform (DWT)-based search algorithm, are implemented on hardware (i.e., FPGA device on Cray XD1 reconfigurable computer that is 10 times faster than software implementation). Niu Li-pi with his team

[34] proposed a multi-sensor image registration approach based on edge-correlation.

III. CORRELATION COEFFICIENT

The CC is a statistical measure of how well the trends in the predicted values follow the trends in the past actual values. It is a measure of how well predicted values from a forecast model “fit” with the real-life-data. As the strength of relationship between the predicted values and actual values increases, so does CC. Thus higher CC is better.

$$C(t,s,\theta) = \frac{\sum_x \sum_y [I_1^{new}(x,y) - \overline{I_1^{new}(x,y)}] [I_2^{new}(x \cos \theta - y \sin \theta - t, x \sin \theta + y \cos \theta - s) - \overline{I_2^{new}(x,y)}]}{\sqrt{\sum_x \sum_y [I_1^{new}(x,y) - \overline{I_1^{new}(x,y)}]^2 \sum_x \sum_y [I_2^{new}(x \cos \theta - y \sin \theta - t, x \sin \theta + y \cos \theta - s) - \overline{I_2^{new}(x,y)}]^2}} \quad (1)$$

I_1^{new}, I_2^{new} - Two new images that differ from each other by rotation and translation only.

t, s - Shifting parameters between the two images.

θ - Rotation angle.

$\overline{I_1^{new}(x,y)}, \overline{I_2^{new}(x,y)}$ - Average structure value of the pixels in overlapping parts of images $I_1^{new}(x,y), I_2^{new}(x,y)$ respectively.

Intuitively, Correlation Coefficient measures the information that X and Y share: it measures how much similar one of these variables are about the other or dissimilar about the other. For example, if X and Y are independent, then no relationship between X and Y and vice versa, so their correlation coefficient is zero. At the other extreme, if X and Y are identical then all information in X is similar to Y and vice versa.

Correlation Coefficient is used in medical imaging for image registration. Given a reference image (for example, a brain scan), and a second image which needs to be put into the same coordinate system as the reference image, this image is deformed until the correlation coefficient between it and the reference image is maximized.

IV. METHODOLOGY

A. Walsh Transform

The Walsh, Haar [13], etc are examples of orthogonal transforms. The coefficients of such an extension point toward the effectiveness of the occurrence of analogous structure at the particular position. These coefficients are normalized by dc coefficient of the expansion, i.e., local average gray value of image, then measure purely local structure independent of modality. Walsh basis functions correspond to local structure, in the form of positive or negative going horizontal or vertical edge, corner of a certain type, etc. In addition, registration schemes based on wavelet coefficient matching do not present general mechanism of combining matching results across different scales.

Two images I_1 and I_2 , I_1 is assumed as reference image and I_2 as an image that has to be deformed to match I_1 . Consider around each pixel, excluding border pixels, 3X3 neighborhood and compute from it, nine Walsh coefficients (3X3 WT of a 3X3 image patch). If ‘ f ’ is input image, matrix

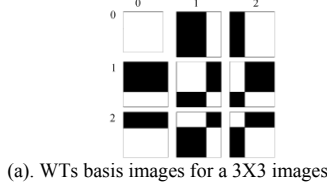
of coefficients 'g' computed for it using equation (2),

$$g = (W^{-1})^T . fW^{-1} \quad (2)$$

Matrix contains coefficients of expansion of the image, in terms of basis images formed by taking vector outer products of the rows of matrix W and its inverse W^{-1} . These basis images are shown in Fig. 1(a). These coefficients are denoted by $a_{00}, a_{01}, a_{02}, a_{10}, a_{11}, a_{12}, a_{20}, a_{21}, a_{22}$, and in a matrix form as shown in Fig. 1(b). These coefficients take value in the range [0, 9]. Moreover normalization given by equation (3) makes method robust to global levels of change of illumination.

$$\alpha_{ij} = a_{ij} / a_{00} \quad (3)$$

However, information having dense features and rigid body transformation allows for plenty of redundancy in the system and makes it robust to noise and bad matches of individual pixels which effectively represent lack of local information. One may construct a unique number out of eight numbers if one uses these numbers as digits of the unique number. Number of levels depends on number system adopted. For decimal system, the normalized coefficients are quantized so that they take integer values in the range [0, 9].



a_{00}	a_{01}	a_{02}
a_{10}	a_{11}	a_{12}
a_{20}	a_{21}	a_{22}

(b). Nine coefficients in matrix form
Figure 1. Walsh Transformation

In Figure 1(a) coefficients along the first row and first column are of equal importance, as they measure the presence of a vertical or horizontal edge, respectively. The remaining four coefficients measure presence of a corner.

The following ordering of coefficients are used in images,

Ordering IA $\alpha_{01}, \alpha_{10}, \alpha_{20}, \alpha_{02}, \alpha_{11}, \alpha_{21}, \alpha_{12}, \alpha_{22}$

Ordering IB $\alpha_{10}, \alpha_{01}, \alpha_{02}, \alpha_{20}, \alpha_{11}, \alpha_{12}, \alpha_{21}, \alpha_{22}$

Ordering IIA $\alpha_{22}, \alpha_{21}, \alpha_{12}, \alpha_{11}, \alpha_{02}, \alpha_{20}, \alpha_{10}, \alpha_{01}$

Ordering IIB $\alpha_{22}, \alpha_{12}, \alpha_{21}, \alpha_{11}, \alpha_{20}, \alpha_{02}, \alpha_{01}, \alpha_{10}$

B. Fast Walsh Hadamard Transform

A fast transform algorithm can be considered as a sparse factorization of the transform matrix, and refer to each factor as a stage. The proposed algorithms have regular interconnection pattern between stages, and consequently, inputs and outputs for each stage are addressed from or to same positions, and the factors of decomposition, stages, have property of being equal between them. The 2X2 Hadamard matrix is defined as H_2 by equation (4) as

$$H_2 = \begin{bmatrix} 1 & 1 \\ 1 & -1 \end{bmatrix} \quad (4)$$

A set of radix-R factorizations in terms of identical sparse matrices can be rapidly obtained from FWHT property that relates matrix H with its inverse and is given in equation (5),

$$HR^n = R^n (HR^n)^{-1} \quad (5)$$

Where HR^n = radix-R Walsh Hadamard transform;

R^n = radix-R factorizations;

n = input element;

The FWHT is utilized to obtain local structure of images. This basis function can be effectively used to obtain digital numbers in the sense of coefficients [18] [19]. If these coefficients are normalized by dc coefficient of expansion, i.e., local average gray value of image, then they measure purely local structure independent of modality. These numbers are then normalized to obtain a unique number. This is used as feature for image registration. The FWHT comparing with WT readily reduces time consumption for medical image registration.

V. RESULTS

A series of experiments is performed using medical images. The tests are performed using different images of different sizes. A set of CT and magnetic resonance (MR) medical images which depict the head of the same patient is considered. The original size of these images is given as pixels. In order to remove the background parts and the head outline, the original images are cropped, creating sub-images of different dimension pixels.

A. Monomodal Brain Image Registration

Consider a CT Sagittal Image – 432 x 427 – 41k JPEG , 36.3kB for registration. During image registration, figure 2, (a) the registered image is same for both WT & FWHT. Also figure 2.(b) shows that base 1 of both WT & FWHT gives the same difference in images.

Table 1 show the summary of all the results taken into account using WT and FWHT in terms of CC. CC represents Correlation Coefficient. Figure 4 shows the performance comparison of WT and FWHT with respect to CC.

1) CT Sagittal Image – 432 x 427 – 41k JPEG , 36.3kB



(a) Registered Image obtained using WT



b) Difference in images obtained using WT

Figure 2. Images obtained using WT



a) Registered Image obtained using FWHT



b) Difference in images obtained using FWHT

Figure 3. Images obtained using FWHT

TABLE 1. REPRESENTS RESULTS FOR CONVENTIONAL WT, AND FWHT USING CC

S.No	X in mm	Y in mm	Angle in degrees	CC after registration For WT	CC after registration for FWHT
1	4	-10	9	0.6451	0.6324
2	-12	-7	13	0.5596	0.5546
3	5	-7	5	0.7383	0.6846
4	-14	-15	2	0.6012	0.5197
5	-8	-7	1	0.3901	0.7909
6	9	7	-7	0.7509	0.7601
7	7	-13	11	0.6335	0.5948
8	18	1	19	0.6020	0.5702
9	-17	0	-17	0.5835	0.5996
10	0	-9	12	0.2256	0.6075
11	23	-6	2	0.6175	0.5373
12	-15	5	-10	0.6723	0.6437
13	22	20	2	0.5904	0.4967
14	5	15	12	0.6647	0.6250
15	-21	16	-5	0.5650	0.5126
16	-1	19	13	0.6226	0.6028
17	5	10	-25	0.5343	0.4986
18	-3	11	25	0.5286	0.5198
19	11	-9	0	0.8197	0.8503
20	0	0	12	0.6108	0.5977
21	0	0	0	0.9797	0.9998

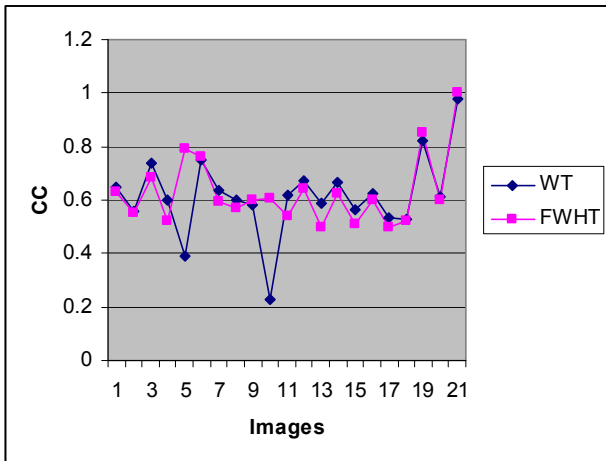


Figure 4. Comparison of WT and FWHT using CC.

B. Multimodal Brain Image Registration

For the evaluation of the algorithm, 6 such sets of MR and CT image pairs are considered. Table 2 show the summary of all the results taken into account using WT and FWHT in terms of CC. X, Y represents the translated points, Θ represents the rotation angle, and CC represents Correlation Coefficient [15].

Table 2 show the summary of all the results taken into account using WT and FWHT in terms of CC. CC represents Correlation Coefficient. Figure 17 shows the performance comparison of WT and FWHT with respect to CC.

- 1) *Sagittal 840 x 754 - 69k - jpg CT & Sagittal 500 x 500 - 72k - jpg MRI - WT*



Figure 5a) Registered Image obtained using WT

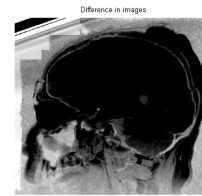


Figure 5b) Difference in images obtained using WT

- 2) *Sagittal 840 x 754 - 69k - jpg CT & Sagittal 500 x 500 - 72k - jpg MRI - FWHT*



Figure 6a) Registered Image obtained using FWHT



Figure 6b) Difference in images obtained using FWHT

- 3) *Sagittal 500 x 500 - 72k - jpg MRI & Sagittal 840 x 754 - 69k - jpg CT - WT*



Figure 7a) Registered Image obtained using WT



Figure 7b) Difference in images obtained using WT

- 4) *Sagittal 500 x 500 - 72k - jpg MRI & Sagittal 840 x 754 - 69k - jpg CT - FWHT*



Figure 8a) Registered Image obtained using FWHT



Figure 8b) Difference in images obtained using FWHT

- 5) *Axial 320 x 420 - 40k - jpg CT & Axial 553 x 642 - 38k - jpg-MRI - WT*

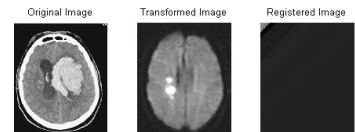


Figure 9a) Registered Image obtained using WT



Figure 9b) Difference in images obtained using WT

6) Axial 320 x 420 - 40k - jpg CT & Axial 553 x 642 - 38k - jpg-MRI - FWHT



Figure 10a) Registered Image obtained using FWHT

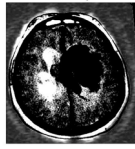


Figure 10b) Difference in images obtained using FWHT

7) Axial 553 x 642 - 38k - jpg-MRI & Axial 320 x 420 - 40k - jpgCT - WT

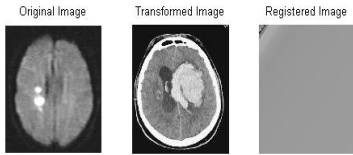


Figure 11a) Registered Image obtained using WT



Figure 11b) Difference in images obtained using WT

8) Axial 553 x 642 - 38k - jpg-MRI & Axial 320 x 420 - 40k - jpgCT - FWHT

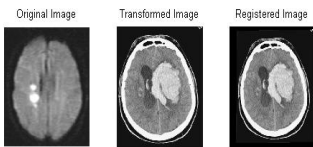


Figure 12a) Registered Image obtained using FWHT



Figure 12b) Difference in images obtained using FWHT

9) Sagittal 432 x 427 - 41k - jpg- CT & Frontal 400 x 400 - 18k - jpg- MRI - WT



Figure 13a) Registered Image obtained using WT



Figure 13b) Difference in images obtained using WT

10) Sagittal 432 x 427 - 41k - jpg- CT & Frontal 400 x 400 - 18k - jpg- MRI - FWHT

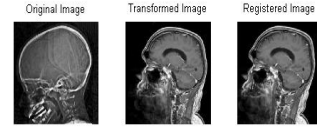


Figure 14a) Registered Image obtained using FWHT

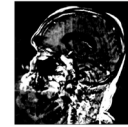


Figure 14b) Difference in images obtained using FWHT

11) Frontal 400 x 400 - 18k - jpg- MRI & Sagittal 432 x 427 - 41k - jpg- CT- WT

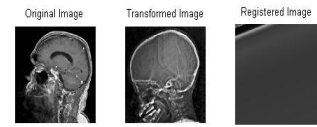


Figure 15a) Registered Image obtained using WT



Figure 15b) Difference in images obtained using WT

12) Frontal 400 x 400 - 18k - jpg- MRI & Sagittal 432 x 427 - 41k - jpg- CT- FWHT



Figure 16a) Registered Image obtained using FWHT



Figure 16b) Difference in images obtained using FWHT

TABLE 2. REPRESENTS RESULTS FOR WT & FWHT USING CC

S. No	CC after registration for Walsh Transform	CC after registration for Fast Walsh Hadamard Transform
1	-0.0459	0.5330
2	0.1838	0.4429
3	0.0130	0.6752
4	-0.0498	0.7483
5	-0.0557	0.5452
6	-0.0837	0.5638

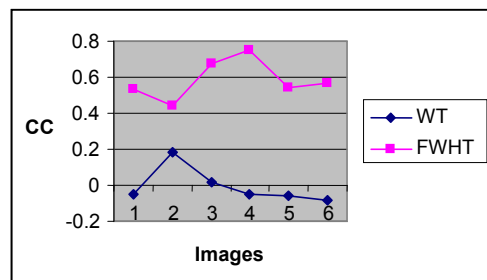


Figure 17. Comparison of WT & FWHT using CC.

VI. CONCLUSION

Correlation Coefficient measure was presented as similarity metric for CT/ MRI registration. This method was validated by medical image CT and MRI with different size and different level noise using Walsh Transform and Fast Walsh Hadamard Transform. This metric is more accurate and efficient. It is a good method to evaluate the accuracy of registration. The registration scheme is easy to implement and it does not require estimating probability densities at every iteration. The experiments show that the method is not sensitive to geometrical distortion, intensity inhomogeneity and data missing. Though it is said that no intervention is needed, from the experiments it proves that proper strategies in sampling and visual inspection are both necessary to avoid local extreme and large errors. The results demonstrate that subvoxel multimodal registration accuracy has to be achieved using the maximization of correlation coefficient, which makes this method very well suited for clinical applications. Future work is to apply the parameters for the image contrast, image fusion after registration, motion detection and target recognition and also to investigate a faster algorithm in order to make the registration more robust and more efficient. Results proved that good accuracy and robustness can be obtained by using Correlation Coefficient method in image registration. Besides, the method significantly improved matching errors which are caused by the individual use of correlation coefficient. Here Correlation Coefficient for Fast Walsh Hadamard Transform is to be maximized hence it is to be combined with the Mutual Information ratio that may also improve registration where both global and local searches are required.

REFERENCES

- [1] George K. Matsopoulos, Nicolaos A. Mouravliansky, Konstantinos K. Delibasis, and Konstantina S. Nikita, "Automatic Retinal Image Registration Scheme Using Global Optimization Techniques," *IEEE Transactions on Information Technology in Biomedicine*, vol. 3, no. 1, pp. 47-60, 1999.
- [2] G. Wolberg, and S. Zokai, "Robust image registration using log-polar transform," *Proceedings of International Conference on Image Processing*, vol. 1, pp. 493-496, 2000.
- [3] Yang-Ming Zhu, "Volume Image Registration by Cross-Entropy Optimization," *IEEE Transactions on Medical Imaging*, vol. 21, no. 2, pp. 174-180, 2002.
- [4] Jan Kybic, and Michael Unser, "Fast Parametric Elastic Image Registration," *IEEE Transactions on Image Processing*, vol. 12, no. 11, pp. 1427-1442, 2003.
- [5] Y. Bentoutou, N. Taleb, K. Kpalma, and J. Ronsin, "An Automatic Image Registration for Applications in Remote Sensing," *IEEE Transactions on Geosciences and Remote Sensing*, vol. 43, no. 9, pp. 2127-2137, 2005.
- [6] Luciano Silva, Olga R. P. Bellon, and Kim L. Boyer, "Precision Range Image Registration Using a Robust Surface Interpenetration Measure and Enhanced Genetic Algorithms," *IEEE Transactions on Pattern Analysis and Machine Intelligence*, vol. 27, no. 5, pp. 762-776, 2005.
- [7] R. Matungka, Y. F. Zheng, and R. L. Ewing, "Image registration using Adaptive Polar Transform," *15th IEEE International Conference on Image Processing, ICIP 2008*, pp. 2416-2419, 2008.
- [8] G. Khaissidi, H. Tairi and A. Aarab, "A fast medical image registration using feature points," *ICGST-GVIP Journal*, vol. 9, no. 3, 2009.
- [9] Wei Pan, Kaihuai Qin, and Yao Chen, "An Adaptable-Multilayer Fractional Fourier Transform Approach for Image Registration," *IEEE Transactions on Pattern Analysis and Machine Intelligence*, vol. 31, no. 3, pp. 400-413, 2009.
- [10] R. Matungka, Y. F. Zheng, and R. L. Ewing, "Image registration using Adaptive Polar Transform," *IEEE Transactions on Image Processing*, vol. 18, no. 10, pp. 2340-2354, 2009.
- [11] Jr. Dennis M. Healy, and Gustavo K. Rohde, "Fast Global Image Registration using Random Projections," *4th IEEE International Symposium on Biomedical Imaging: From Nano to Macro, ISBI 2007*, pp. 476-479, 2007.
- [12] C. Fookes and A. Maeder, "Quadrature-Based Image Registration Method using Mutual Information," *IEEE International Symposium on Biomedical Imaging: Nano to Macro*, vol. 1, pp. 728-731, 2004.
- [13] J. L. Moigne, W. J. Campbell, and R. F. Cromp, "An automated parallel image registration technique based on correlation of wavelet features," *IEEE Trans. Geosci. Remote Sens.*, vol. 40, no. 8, pp. 1849-1864, Aug. 2002.
- [14] J. P. W. Pluim, J. A. Maintz, and M. A. Viergever, "Image registration by maximization of combined mutual information and gradient information," *IEEE Trans. Med. Imag.*, vol. 19, no. 8, pp. 899-814, Aug. 2000.
- [15] Z. Zhang, J. Zhang, M. Liao, and L. Zhang, "Automatic registration of multi-source imagery based on global image matching," *Photogramm. Eng. Remote Sens.*, vol. 66, no. 5, pp. 625-629, May 2000.
- [16] M. Bossert, E. M. Gabidulin, and P. Lusina, "Space-time codes based on Hadamard matrices proceedings," in *Proc. IEEE Int. Symp. Information Theory*, Jun. 25-30, 2000, p. 283.
- [17] [19] L. Ping, W. K. Leung, and K. Y. Wu, "Low-rate turbo-Hadamard codes," *IEEE Trans. Inf. Theory*, vol. 49, no. 12, pp. 3213-3224, Dec. 2003.
- [18] D.Sasikala and R.Neelaveni, 2010, "Registration of Brain Images using Fast Walsh Hadamard Transform", *International Journal of Computer Science and Information Security*, Vol 8, No:2, pp. 96-105.
- [19] D.R. Sullivan and J.S. Martin, "A Coarse Search Correlation Tracker for Image Registration", *IEEE Transactions on Aerospace and Electronic Systems*, Volume: AES-17, Issue: 1, Jan. 1981, pp 29 - 34.
- [20] M. Holden, J.A. Schnabel and D.L.G. Hill, "Quantification of small cerebral ventricular volume changes in treated growth hormone patients using nonrigid registration", *IEEE Transactions on Medical Imaging*, Volume : 21 , Issue:10 , Oct. 2002, pp 1292 - 1301.
- [21] J. Inglada and A. Giros, "On the possibility of automatic multisensor image registration", *IEEE Transactions on Geoscience and Remote Sensing*, Volume: 42, Issue: 10, Oct. 2004, pp 2104 - 2120.
- [22] A. Anthony and O. Loffeld, "On search space and search data strategies in image registration", *Proceedings of MTS/IEEE OCEANS*, Vol. 1, 2005, pp 58 - 61.
- [23] G. Lazaridis, and M. Petrou, "Image registration using the Walsh transform", *IEEE Transactions on Image Processing*, Volume: 15, Issue: 8, Aug. 2006, pp 2343 - 2357.
- [24] [26] Lee, Doo-Youl Chun, Yong-Jin Yoon, Je-Bum Lee, Sang-Hee Lee, Suk-Joo Cho, Han-Ku Moon, and Joo-Tae, "Impact of registration error of reticle on total overlay error budget", *Journal of Vacuum Science & Technology B: Microelectronics and Nanometer Structures*, Volume: 24, Issue: 6, Nov 2006, pp 3105 - 3109.
- [25] M. Singh, A. Rajagopalan, C. Zarow, X.-L. Zhang, T.-S. Kim, D. Hwang, A.-Y. Lee and H. Chui, "From Human MRI to Microscopy: Co-registration of Human Brain Images to Postmortem Histological Sections", *IEEE Nuclear Science Symposium Conference Record*, Volume : 4, 2006, pp 1982 - 1985.
- [26] Xiaojin Shi , Yunhua Zhang and Jingshan Jiang, "InSAR Image Registration Using Modified Correlation Coefficient Algorithm", *International Symposium on Antennas, Propagation & EM Theory*, 2006, pp 1 - 4.
- [27] F. Chatelain, J.-Y. Tourneret, J. Inglada and A. Ferrari, "Bivariate Gamma Distributions for Image Registration and Change Detection", *IEEE Transactions on Image Processing*, Volume: 16, Issue: 7, July 2007, pp 1796 - 1806.
- [28] Bing Luo and Jun-Ying Gan, "Inhomogeneous illuminated images registration based on wavelet decomposition", *International Conference on Wavelet Analysis and Pattern Recognition*, July 2009, pp 365 - 368.
- [29] I. Ito, A. Uemura and H. Kiya, "Extension of DCT sign phase correlation to subpixel registration", *International Symposium on Intelligent Signal Processing and Communications Systems*, Feb. 2009, pp 1- 4.

- [32] Jichao Jiao , Baojun Zhao , Jianke Li and Linbo Tang, "A Multi-Stage Astronomical Images Registration Based on Nonsubsampled Contourlet Transform", International Congress on Image and Signal Processing, 2009, pp 1-5.
- [33] Miaoqing Huang , O. Serres, T. El-Ghazawi and G. Newby, "Parameterized hardware design on reconfigurable computers: An image registration case study", Southern Conference on Programmable Logic, 2009, pp 71 - 76.
- [34] Niu Li-pi , Yang Ying-yun , Zhang Wen-hui and Jiang Xiu-hua, "A multi-sensor image registration approach based on edge-correlation", International Conference on Signal Processing Systems, Volume : 2 , 2010, pp V2-36 - V2-40.



D. Sasikala is presently working as Assistant Professor, Department of CSE, Bannari Amman Institute of

Technology, Sathyamangalam. She received B.E.(CSE) from Coimbatore Institute of Technology, Coimbatore and M.E. (CSE) from Manonmaniam Sundaranar University, Tirunelveli. She is now pursuing Phd in Image Processing. She has 11.5 years of teaching experience and has guided several UG and PG projects. She is a life member of ISTE. Her areas of interests are Image Processing, System Software, Artificial Intelligence, Compiler Design.



Dr. R. Neelaveni is presently working as a Assistant Professor, Department of EEE, PSG College of Technology, Coimbatore. She has a Bachelor's degree in ECE, a Master's degree in Applied Electronics and PhD in Biomedical Instrumentation. She has 23 years of teaching experience and has guided many UG and PG projects. Her research and teaching interests includes Applied Electronics, Analog VLSI, Computer Networks, and Biomedical Engineering. She is a Life member of Indian Society for Technical Education (ISTE). She has published several research papers in International and National Journals and Conferences.